

Optical properties of single crystals of some rare-earth trifluorides, 5–34 eV

C. G. Olson, M. Piacentini,* and D. W. Lynch

Ames Laboratory—U. S. Department of Energy, and Department of Physics, Iowa State University, Ames, Iowa 50011

(Received 23 January 1978)

The reflectances of single crystals of the trifluorides of La, Ce, Pr, Nd, Dy, and of polycrystalline GdF₃ were measured in the 10–34-eV region, along with 5–9-eV transmission measurements on films of these materials. Localized $4f \rightarrow 5d, 6s$ transitions on the rare-earth ions give rise to the absorption below 10 or 11 eV. Strong interband absorption gives anisotropic reflectance peaks in the 10–15-eV region, presumably from F⁻ $2p$ valence bands to lanthanide $5d, 6s$ (and other states) conduction bands, accounting for about one-third of the expected F⁻ $2p$ oscillator strength. Transitions from lanthanide $5p$ levels cause two types of spectra beginning around 20 eV: transitions of the $5p \rightarrow 5d$ type, apparently localized on lanthanide ions, but with some anisotropy; and transitions of $5p$ electrons to the conduction band, giving a peak of very high reflectance at energies above 27 eV.

INTRODUCTION

The rare-earth trifluorides are wide-band-gap insulators with properties determined by both the $4f$ electrons localized on the rare earths and the band electrons from both ions. They form a series of compounds possessing only two crystal structures. For the light rare earths, the structure is the LaF₃ structure, hexagonal,¹ or more probably, trigonal,^{2,3} and for the heavier rare earths, the trifluorides have the orthorhombic YF₃ structure.¹ In both structures the rare-earth ions are located in cages of fluoride ions, five in the former structure and nine in the latter, counting those ions with about the same distance as nearest neighbors, even though some are slightly further away than others. The compounds form solid solutions to a considerable extent, and LaF₃ doped with rare earths has been investigated as a possible vacuum uv laser material.^{4,5}

In the following we report on the optical properties in the vacuum ultraviolet of the trifluorides of La, Ce, Pr, Nd, Gd, and Dy. By using single crystals and polarized synchrotron radiation we can study the anisotropy of the optical properties. In the energy range investigated, the spectra are determined by valence-to-conduction-band transitions, as well as transitions from the rare-earth $4f$ and $5p$ core levels. Since band structures are lacking, a preliminary interpretation based on atomic levels and binding considerations is presented, but it also explains the anisotropy of the interband absorption. Transitions from the $5p$ levels are seen to consist of highly localized atomiclike transitions and transitions to bandlike final states. A preliminary report of our data for LaF₃ and PrF₃ has been given previously,⁶ but several aspects of that report will be altered in what follows. Vacuum ultraviolet reflectances of

films of LaF₃, CeF₃, PrF₃, and NdF₃ have been presented by Stephan *et al.*^{7,8} Their results will be discussed along with our own.

EXPERIMENTAL

Single crystals of the trifluorides of La, Ce, Pr, Nd, and Dy and a large polycrystalline sample of GdF₃ were obtained.⁹ The single crystals were cut with the c axis either in or normal to the face of the sample, except for DyF₃, which was un-oriented. The samples were cut with a diamond saw, lapped on SiC paper and polished with Al₂O₃ abrasives in water, finishing with 0.05- μ m-diameter particles. Care was taken to reduce surface damage by polishing only until scratch marks from the previous grit were removed. There were a number of small pits on the surface of most crystals. These seemed to arise from internal strains, for the only samples free of them were some of NdF₃, and these crystals were the only ones exhibiting no internal cracks in samples polished on both sides for transmission measurements in the visible and near uv. All polished single crystals yielded good back-reflection Laue x-ray diffraction patterns. Films of each salt were evaporated on polished LiF for transmission measurements to about 10.5 eV.

The measurements of reflectance at 10° from normal incidence were made in a sample chamber previously described.¹⁰ Synchrotron radiation from the 240-MeV electron storage ring at the Physical Sciences Laboratory of the University of Wisconsin was the light source. The radiation at the sample was at least 88% polarized.

Measurements of the reflectance of LaF₃ could be made below 10 eV, in the region of transparency. The other rare-earth trifluorides could not be so measured in this region, for there is

absorption involving the excitation of the $4f$ electrons that leads to intense luminescence, detected along with the reflected beam. This luminescence has been studied in CeF_3 .⁵ (The reflectance of PrF_3 given in Ref. 6 is in error below 10 eV because of luminescence.) This region was studied by measuring the transmission of thin films on LiF , which did not luminesce enough to cause errors.

Errors due to second-order and scattered radiation were negligible. The principal error is in the quality of the sample surface—how close to ideal is the surface. Errors due to surface roughness and pits may be estimated, but not those due to strains. The sample-to-sample repeatability in the heights of the reflectance peaks is about ± 0.03 . As indicators of anisotropy, the number of peaks and the positions of single peaks are reliable, but the relative heights of peaks in the spectra for \vec{E} parallel to and \vec{E} perpendicular to \hat{c} may not be, for peak-height anisotropies could result from the effect of the anisotropy of the mechanical properties of the crystal on the polishing process.

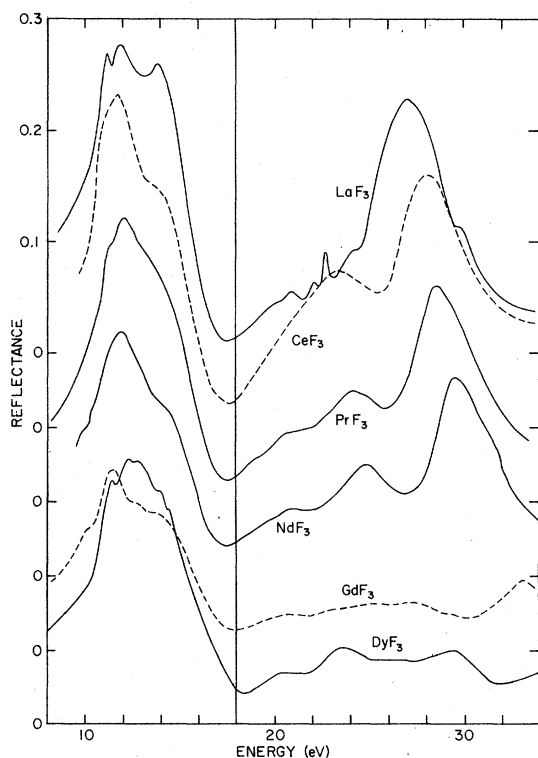


FIG. 1. Reflectances of several rare-earth trifluorides. For LaF_3 , CeF_3 , PrF_3 and NdF_3 , the basal-plane reflectance is shown. That of DyF_3 is from an unoriented single crystal while that for GdF_3 is from a polycrystalline sample.

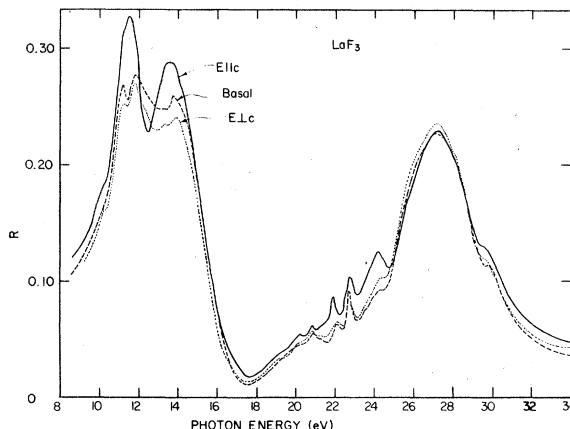


FIG. 2. Reflectances of single-crystal LaF_3 .

RESULTS

An overview of the reflectances is given in Fig. 1, which shows a reflectance spectrum for each salt measured. The detailed single-crystal reflectances are shown in Figs. 2-6. The reflectances of thin film samples measured by Stephan *et al.*^{7,8} are a mixture of $\vec{E} \parallel \hat{c}$ and $\vec{E} \perp \hat{c}$ spectra, and have peaks between 10 and 15 eV, generally in good agreement with those reported here. The principal difference is that our peak heights are about 0.28-0.30, while the film reflectances peak at about 0.22, and that the film spectra always show three peaks in this region, while our data do not always have the three resolved. (As mentioned below, we expect that there are three peaks for $\vec{E} \perp \hat{c}$ in all salts studied.) The large peak at high energy has a reflectance of 0.23 in our data, and 0.12 in the film reflectance, and there are some discrepancies of up to about 1 eV in the peak positions. Finally, in the region 20-25 eV

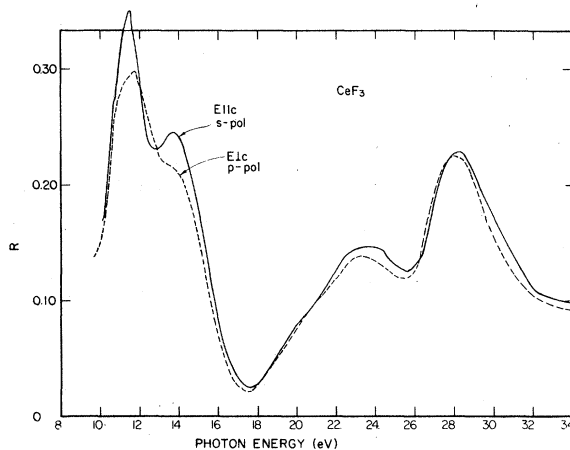


FIG. 3. Reflectances of a single crystal CeF_3 .

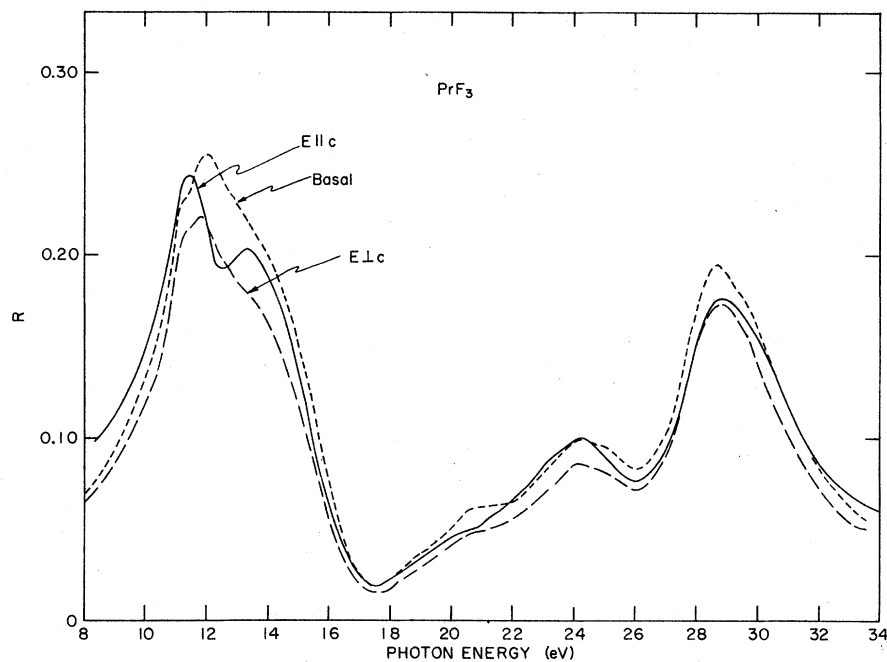


FIG. 4. Reflectances of a single crystal PrF_3 .

there are a number of small peaks. In some cases we have resolved more peaks with single crystals than were seen on films, but CeF_3 and PrF_3 show fewer. These two salts also have less-well-resolved spectra at 10–15 eV, and probably are rather strained.

The weak structures between 20 and 25 eV are

well resolved in LaF_3 , but not in the other crystals. This was at first believed to be the result of poor surface quality of all the crystals, except LaF_3 , but that is not the case. We examined a large number of NdF_3 crystals to try to improve the resolution. These included a crystal that had been annealed 18 h at 600°C in Ar, one

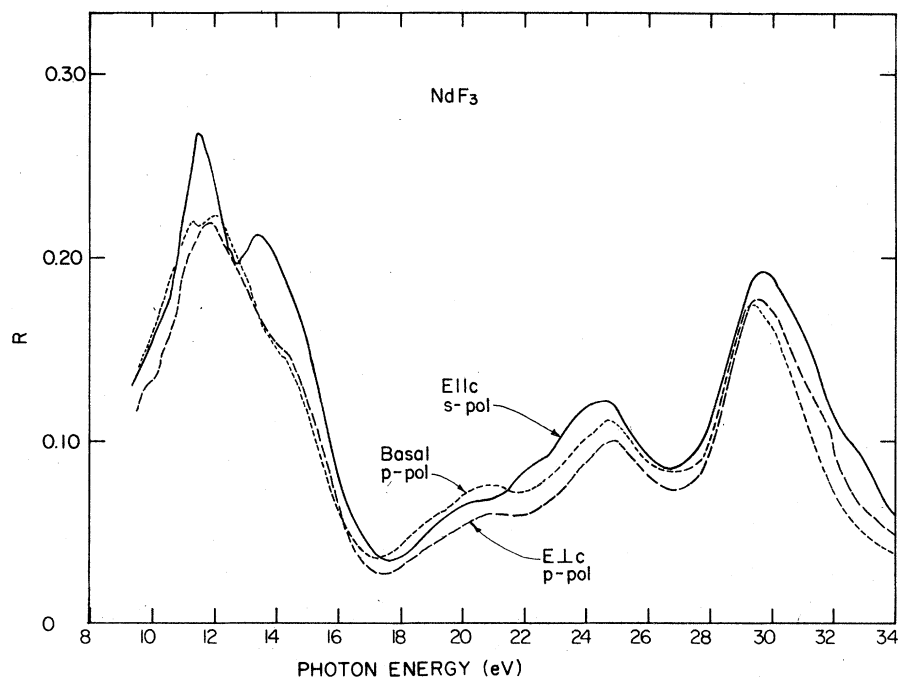


FIG. 5. Reflectance of single crystal NdF_3 .

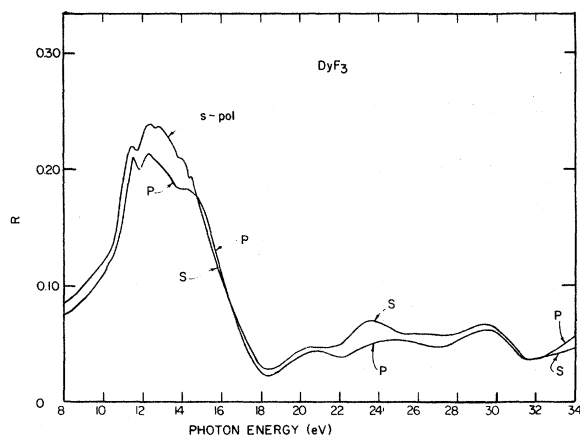


FIG. 6. Reflectance of an unoriented single crystal DyF_3 . The two curves represent not only different polarizations with respect to the plane of incidence, but also with respect to crystal axes in the unoriented single crystals.

that had been etched¹¹ in a solution of $\text{Al}(\text{NO}_3)_3$, and the free surface of the solidified melt, i.e., a surface that had not been cut, lapped, or polished. We also made transmission measurements on a film of NdF_3 evaporated on an unsupported Al film with a very thin Au layer to keep the NdF_3 from reacting with the Al during evaporation. None of these produced spectra that were any better resolved than those of Fig. 5. Nonetheless, sometimes reflectance spectra of films have produced better-resolved structures.^{7,8} The transmission spectra of thin films of several rare-earth trifluorides are shown in Fig. 7.

Stephan *et al.*^{7,8} have Kramers-Kronig (KK) analyzed their reflectance data. The result for LaF_3 is straightforward, but they report some uncertainties for the other salts due to the data in the region below 10 eV. Accurate values of the absorption coefficients below 10 eV, in lieu

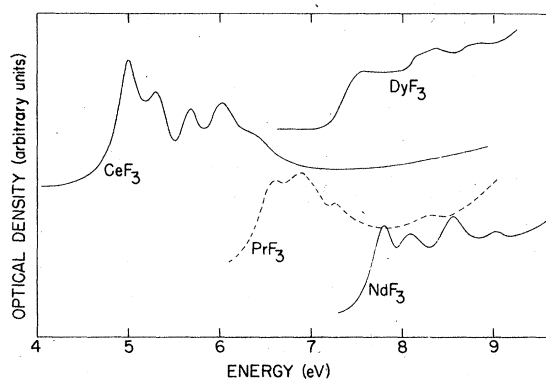


FIG. 7. Optical densities of thin films of CeF_3 , PrF_3 , NdF_3 , and DyF_3 on LiF.

of reflectance data, are needed to do a KK analysis, but these are not available. Moreover, the heavier rare-earth fluorides are expected to show a reflectance peak above our maximum energy, making the high-energy extrapolation difficult. Since the spectra of all the salts are similar above 10 eV, we can take the results of Stephan *et al.*^{7,8} as an aid in interpretation, for one should use conductivity or dielectric function spectra for such purposes, not reflectance spectra. Stephan *et al.*⁷ find that the ϵ_2 spectrum of LaF_3 resembles that of the reflectance in the shapes and, less quantitatively, in the relative heights of structures. There probably is some shift in the peak positions below 20 eV or so between the two spectra, but this is difficult to read from their figures. To assess oscillator strengths, a fit to a series of harmonic oscillators was made for PrF_3 and the partial sum rule on ϵ_2 was evaluated.

Some rudimentary luminescence excitation spectra were made on LaF_3 , CeF_3 , and PrF_3 , and $\text{La}_{0.5}\text{Pr}_{0.5}\text{F}_3$. The exciting radiation was from the monochromator, but with a LiF filter to remove second-order radiation, and the emission was measured through a glass window. (No emission of higher-energy photons occurred.) Thus only radiation from the excited $4f$ manifold was measured. The spectra for PrF_3 and $\text{La}_{0.5}\text{Pr}_{0.5}\text{F}_3$ resembled the absorption of PrF_3 shown in Fig. 7, as expected from the work of Elias *et al.*⁴ Upon removing the LiF filter and scanning to higher energies, a broad minimum in excitation efficiency was found at 17.5 eV, and then a peak at about 22 eV was found. No luminescence could be detected upon excitation near the reflectance peak at 29 eV. The only luminescence detected in LaF_3 was excited in the 6–10-eV region, and presumably was due to rare-earth impurities, probably Ce. The small shoulders on the reflectance spectra in Figs. 2, 5, and 6 may be the result of luminescence rather than reflectance structures. Luminescence excited in the 12–13-eV region may be responsible for the apparent loss of structure in the 10–15-eV region of some of our spectra.

DISCUSSION

$4f$ excitations

The $4f$ - $4f$ transitions that give these compounds their characteristic colors occur at energies lower than those used here.^{12,13} They are too weak to be seen easily in thin films. The lowest-energy features of concern here are those of Fig. 7. LaF_3 , lacking $4f$ electrons, exhibits no absorption below 10 eV.¹⁴⁻¹⁶ From the energies

and strengths of the peaks between 5 and 10 eV and from knowledge of the free rare-earth ion spectra,¹⁷ these bands are assigned to the $4f-5d$ transitions on the rare-earth ions. These transitions lie about 1 eV lower in energy in the crystal than in the free ion, an effect of the crystal potential on the final states. The corresponding transitions have been observed by Elias *et al.*⁴ for rare earths as impurities in LaF_3 , in which case the transitions occur at nearly the same energy as in the pure rare-earth trifluorides, but the bands are somewhat sharper. In the work of Elias *et al.* there was a pronounced sharpening of the bands upon cooling, showing that at least the final state interacts appreciably with the lattice. The lowest $4f-5d$ transitions have also been observed for rare-earth impurities in CaF_2 .^{18,19} In LaF_3 the splitting of the impurity $4f-5d$ transitions is much larger than the expected spin-orbit splitting of the levels involved, so crystal-field splitting dominates.⁵ With the low symmetry of the rare-earth ion site (C_2), five transitions are expected, and this is usually what is observed. X-ray-induced photoemission spectra²⁰ show that the rare-earth $4f$ levels drop with increasing atomic number at about the same rate at which the first moments of the absorption structures in Fig. 7 increase. (For Dy, a second group of $4f$ levels becomes occupied,²⁰ and the absorption shown for DyF_3 in Fig. 7 is from these levels, not the deeper set.)

The excitation of the $4f-5d$ transitions in Ce-doped LaF_3 or in CeF_3 itself causes broad-band fluorescence with a Stokes shift.⁵ The excited state of the Ce^{+3} ion clearly interacts with the lattice. The lifetime for this allowed emission is 20 nsec. The corresponding absorption by Pr in LaF_3 gives a different emission spectrum, one consisting of sharp lines. The excited $5d$ state loses energy rapidly to an excited state of the $4f^2$ configuration, which emits the line fluorescence with a lifetime of 720 nsec.⁵

The $4f-6s$ transitions occur at higher energy in the free rare-earth ions,¹⁴ and are stronger than the $4f-5d$. There is nothing special in the reflectance spectra of the rare-earth trifluorides that can be assigned to them. They presumably underlie the strong absorption between 10 and 15 eV, but this absorption is nearly the same for all salts studied, including LaF_3 , which has no $4f$ electrons. The $4f-6s$ absorption is probably too weak to be seen in the presence of the 10–15-eV absorption. (There is also the possibility that there may be some manifestation of it in the 9–10-eV region, a region difficult to study in reflectance on single crystals.) Such transitions can also be found by luminescence excitation studies. Elias *et al.*⁴

report that $4f-6s$ absorption begins at ~7.7 and 9.5 eV for Ce^{3+} and Pr^{3+} , respectively, doped into LaF_3 . The former is not evident in our Fig. 7, while the latter falls in the region just discussed, and $4f$ manifold luminescence can be excited in this region in PrF_3 .

Valence-band excitations

The strong reflectance peaks at 10–14 eV are not due to transitions localized on or around rare-earth ions. They occur at about the same energy in all the salts studied here and appear nearly the same in all of them, even when the crystal structure changes. Since there have been no band calculations for any lanthanide trifluoride, we can achieve only a qualitative picture of the excitation spectrum.

Consideration of free-ion levels¹⁷ and the Madelung potential²¹ places the $F^- 2p$ levels some 10 eV below (lanthanide)³⁺ $5d$ and $6s$ levels. The former atomic levels become the valence band, as they do in alkali and alkaline-earth fluorides, and the latter, perhaps mixed with $F^- 3s$ states and other lanthanide states, become the conduction band. For the moment, we neglect the very localized empty lanthanide $4f$ states, since the oscillator strength for transitions from the $F^- 2p$ valence bands is likely to be very weak. The ionic levels split under the influence of the uniaxial crystal field, and symmetry considerations will help to construct an energy-level sequence for the bands. Although the actual unit cell has trigonal symmetry and six molecules, we shall make use of the simpler hexagonal unit cell with only two molecules. We should not be misled much by this simplification, for it has been difficult to distinguish the two experimentally in LaF_3 .^{2,3} The states of the D_{6h}^4 space group transform as representations of the point group D_{6h} at the center of the Brillouin zone. In Table I we give the symmetrized combinations of Bloch functions at the point Γ for $F^- s$ and p states and lanthanide s , p , d , and f states.

Consider first the conduction bands. Combinations with bonding character of the $6s$ and $5d$ lanthanide states, transforming as even representations in Table I, lie at lower energies than their antibonding counterparts. In addition, the combinations of xz and yz d -functions are pushed downwards with respect to the other orbitals that do not contain a z component because of electrostatic energy. Probably the bottom of the conduction band is a Γ_1^+ state with some s character, which shows more dispersion than the more localized d bands. Electric dipole transitions to these s and d states are allowed only from odd-

TABLE I. Symmetrized combinations of Bloch functions derived from La^{3+} s , p , d , and f states and F^- s and p states, for the LaF_3 hexagonal cell (Ref. 1) at the point Γ of Brillouin zone. The positions of the ions in the unit cell (Ref. 1) are also given. Except for the s states, Cartesian expressions for the angular momentum functions have been used. The combinations of orbitals centered on inequivalent ions in the unit cell are explicitly indicated, while summation over all cells is implicit. The subscripts used to identify the ions on which the orbitals are centered correspond to those given at the top of the table, e.g., $z_{\bar{B}}$ is a p_z orbital. Irreducible representations are labeled according to J. C. Slater *Quantum Theory of Molecules and Solids* (McGraw-Hill, New York 1965), Vol. II.

Position of atoms in the unit cell ($a=4.148 \text{ \AA}$, $c_0=7.354 \text{ \AA}$)					
La^{3+} ($2c$): $A: (\frac{2}{3}, \frac{1}{3}, \frac{1}{4})$; $B: (\frac{1}{3}, \frac{2}{3}, -\frac{1}{4})$					
F^- ($4f$): $A^+: (\frac{2}{3}, \frac{1}{3}, -0.43)$; $B^-: (\frac{1}{3}, \frac{2}{3}, 0.43)$					
$A^-: (\frac{2}{3}, \frac{1}{3}, -0.07)$; $B^+: (\frac{1}{3}, \frac{2}{3}, 0.07)$					
F^- ($2b$): $A^0: (0, 0, \frac{1}{4})$ $B^0: (0, 0, -\frac{1}{4})$					
s states		d states		f states	
$s_A \pm s_B$	Γ_1, Γ_4	$(3z^2 - r^2)_A \pm (3z^2 - r^2)_B$	Γ_1^+, Γ_4^-	$x(x^2 - 3y^2)_A \pm x(x^2 - 3y^2)_B$	Γ_4^-, Γ_1^+
p states		$(xy)_A \pm (xy)_B$	Γ_5^+, Γ_6^-	$x(3x^2 - y^2)_A \pm y(3x^2 - y^2)_B$	Γ_3^-, Γ_2^+
		$(x^2 - y^2)_A \pm (x^2 - y^2)_B$		$z(5z^2 - 3r^2)_A \pm z(5z^2 - 3r^2)_B$	Γ_2^-, Γ_3^+
$z_A \pm z_B$	Γ_2^-, Γ_3^+	$(xz)_A \pm (xz)_B$	Γ_6^+, Γ_5^-	$x(5z^2 - r^2)_A \pm x(5z^2 - r^2)_B$	Γ_6^-, Γ_5^+
$x_A \pm x_B$	Γ_6^-, Γ_5^+	$(yz)_A \pm (yz)_B$		$y(5z^2 - r^2)_A \pm y(5z^2 - r^2)_B$	
$y_A \pm y_B$					$z(x^2 - y^2)_A \pm z(x^2 - y^2)_B$
				$(xyz)_A \pm (xyz)_B$	
s states		p states			
$s_A^0 \pm s_B^0$	Γ_1^+, Γ_4^-	$z_A^0 \pm z_B^0$	Γ_2^-, Γ_3^+	$(z_A^+ + z_A^-) \pm (z_B^+ + z_B^-)$	Γ_2^-, Γ_3^+
$(s_A^+ + s_A^-) \pm (s_B^+ + s_B^-)$	Γ_1^+, Γ_4^-	$x_A^0 \pm x_B^0$	Γ_6^-, Γ_5^+	$(z_A^+ - z_A^-) \pm (z_B^+ - z_B^-)$	Γ_1^+, Γ_4^-
$(s_A^+ - s_A^-) \pm (s_B^+ - s_B^-)$	Γ_2^-, Γ_3^+	$y_A^0 \pm y_B^0$		$(x_A^+ + x_A^-) \pm (x_B^+ + x_B^-)$	Γ_6^-, Γ_5^+
				$(y_A^+ + y_A^-) \pm (y_B^+ + y_B^-)$	
				$(x_A^+ - x_A^-) \pm (x_B^+ - x_B^-)$	Γ_6^+, Γ_5^-
				$(y_A^+ - y_A^-) \pm (y_B^+ - y_B^-)$	

parity states.

In an ionic crystal of noncubic symmetry, crystal-field splitting of the valence band is expected to dominate the F^- $2p$ spin-orbit splitting of only 0.05 eV. Moreover, there are two nonequivalent lattice sites for the F^- ions, assuming the hexagonal structure for LaF_3 , whose electrostatic potentials differ by 0.30 eV,²¹ leading to additional valence bandwidth. The valence bands are expected to split into two main groups of bands, for the F^- $2p$ orbitals centered on the inequivalent sites may point in directions that either do or do not contain a (lanthanide)³⁺ ion. A further splitting for each subband arises from bonding and antibonding combinations of the states, mostly between the p_x and the $p_x p_y$ bands, the former lying at higher energies. In Fig. 8(a) we show an energy-level diagram of the states at Γ construc-

ted on the basis of the previous considerations, and the dipole-allowed transitions between these levels for both polarizations. Only the states of interest for interpreting the valence-band spectra of the rare-earth trifluorides are shown. The three transitions allowed for $\vec{E} // \hat{c}$ are labeled with greek letters, while those for $\vec{E} \perp \hat{c}$ have roman letters. Note that the number of transitions indicated in Fig. 8(a) matches the number of structures in the reflectance spectrum of LaF_3 for both polarizations. The energy splittings between the levels can be obtained by fitting the energies of the reflectivity peaks. This procedure may seem rather arbitrary, since the level diagram shown in Fig. 8(a) is for the point Γ . In general, unless exciton formation occurs, reflectivity peaks are associated with peaks of the joint density of states involving large regions of the

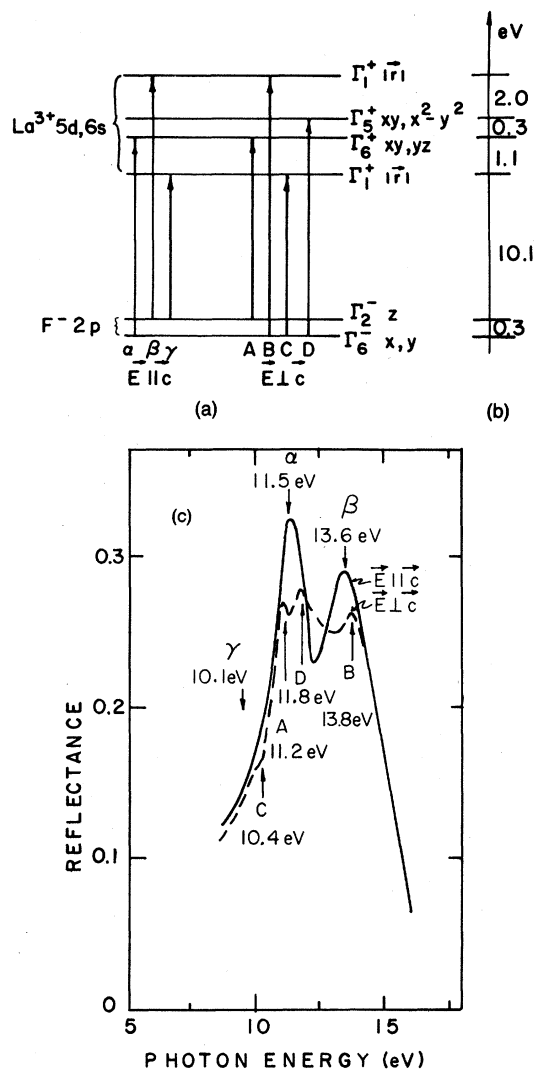


FIG. 8. Schematic transitions at the Brillouin-zone center from a valence band composed of $F^{-} 2p$ functions to a conduction band based on $La^{3+} 5d$ and $6s$ functions, including polarization selection rules (a). Part (b) shows the splittings obtained by fitting the LaF_3 spectra (c).

Brillouin zone. In the present case, at general points of the Brillouin zone, the doubly degenerate levels split by an unknown amount and the selection rules are relaxed. But transitions that are forbidden at Γ and at other symmetry points usually have a small matrix element at general points of the Brillouin zone, and their contribution to the optical spectra cannot be observed. Moreover, it is very likely that the valence bands are rather flat and maintain the same features as at Γ . Therefore, we feel safe in using the energy-level diagram proposed in Fig. 8(a), with the caveat that it does not refer at any particular point in the Brillouin zone, but simply represents the

splitting of the energy levels of the two ions under the influence of the crystal field.

The lowest-energy interband transitions occur to a Γ_1^+ state. These should be weak. In LaF_3 , we associate the two shoulders on the steep low-energy reflectivity rise at 10.1 eV ($\vec{E} \parallel \hat{c}$) and 10.4 eV ($\vec{E} \perp \hat{c}$) with the bands γ and C, respectively. Their separation fixes the splitting between the valence Γ_2^- and Γ_6^- states. In the LaF_3 spectrum two other polarization doublets, with the same energy splitting of 0.3 eV, occur at 11.2–11.5 and 13.8–13.6 eV ($\vec{E} \perp \hat{c} - \vec{E} \parallel \hat{c}$). They can be identified with bands α -A (same Γ_6^+ final state) and β -B (same Γ_1^+ final state). The sequence of the bands for each of the three doublets in switching from $\vec{E} \parallel \hat{c}$ to $\vec{E} \perp \hat{c}$ polarization is in perfect agreement with the diagram of Fig. 8(a). The $\vec{E} \perp \hat{c}$ spectrum shows another strong structure at 11.5 eV, which can be associated with band D in Fig. 8(a). This assignment for the LaF_3 spectra is shown in Fig. 8(c), and the energy-level splittings thus obtained are given in Fig. 8(b). The assignments form a consistent picture, but it is not yet proven that the shoulders assigned to Γ_1^+ final states are not the result of luminescence.

The valence bands of LaF_3 and CeF_3 have been studied by x-ray photoemission spectroscopy²² (XPS), and they conform with the above picture. A recent ultraviolet-photoemission-spectroscopy (UPS) study²³ of LaF_3 also is in agreement. The full width at half maximum is about 3 eV, not correcting for the instrumental resolution of about 1 eV, and there is evidence of two components in LaF_3 , split by about 1.5 eV. The lesser-bound component has the greater intensity. This splitting can be associated with the two groups of valence bands discussed previously. The higher subband then splits into the p_z (Γ_2^-) and p_x, p_y (Γ_6^-) bands shown in Fig. 8(a). Only the electrons lying in these bands contribute significantly to the optical transitions between 10 and 15 eV. In fact, the reflectance data show no structures split by the known 1.5-eV valence-band splitting. Moreover, the f -sum rule saturates at about six electrons per molecule at about 15 eV, as many electrons as the bands shown in Fig. 8(a) can accommodate.

An additional complication is the mixing of the rare-earth $4f$ levels with valence-band states as the former drop in energy with increasing atomic number. XPS measurements^{20,24} show that the degeneracy does not occur before Sm in the rare-earth series, and that for GdF_3 the $4f$ levels are anomalously low and do not overlap the valence bands. Only DyF_3 , of all our crystals, has serious overlap of the two sets of states, but XPS spectra²⁴ indicate that there is little or no interaction be-

tween them, the density of states being additive for the two bands.

Lanthanide 5*p* excitations

The next-deeper levels are the lanthanide 5*p* levels. They lie below the vacuum level by an amount that increases nearly linearly with atomic number²⁵ (for the initial part of the rare-earth series see Ref. 20). They have appreciable spin-orbit splittings, ranging from about 2.3 eV in La and 2.8 eV in Nd to about 4.1 eV in Dy.²⁶ XPS data^{22,24} show these levels clearly. The upper 5*p* level lies about 10 eV (LaF₃) and 11.5 eV (CeF₃) below the peak in the valence-band density of states. The spin-orbit splittings are 2.5 and 3.1 eV, respectively, with the only effect of the crystal being a possible contribution to the observed splitting. There may be an additional contribution to the 5*p* splitting in all our crystals, except LaF₃, arising from exchange coupling of the 5*p* hole with the 4*f* electrons. Such splitting has been observed for 4*s* and 5*s* holes in these salts.²⁷

All rare-earth trifluorides measured show an increase in reflectance (absorption) at about 18 eV, which is the expected threshold for La 5*p* absorption, but which is below that expected for other lanthanides. This absorption probably does not arise from lanthanide 5*p* excitations, but rather from the excitation of valence-band electrons into parts of the conduction band far above the minimum. About one-third of the valence-band oscillator strength has been exhausted by 18 eV in LaF₃. Additional valence-electron absorption underlies the excitation of the lanthanide 5*p* levels. The latter probably cause the relatively sharp structure beginning at 20 eV in LaF₃, and at higher energy in the other trifluorides (Figs. 1-6). The spin-orbit pairs of the lanthanide 5*p* levels should be recognizable, but additional structure due to the final conduction band states, which exhibit crystal-field splitting, may obscure this. The broadening of the spectra precludes finding such pairs, except in LaF₃. The only distinct pair is at 21.9 and 24.2 eV, whose splitting is close to the expected spin-orbit value, and whose behavior upon changing the polarization is the same.

If we consider lanthanide 5*d* and 6*s* final states, we have two initial states, 5*p*_{1/2} and 5*p*_{3/2}, and three final states, 5*d*_{3/2}, 5*d*_{5/2}, and 6*s*_{1/2}. They give rise to five allowed transitions on the free ion. *L-S* coupling is appropriate for the 5*p* → 5*d* transitions and *J-j* coupling for the 5*p* → 6*s*.²⁸ Figure 9 shows these transitions and assigns them as though an atomic picture were valid. Transitions A-C and D-E, are split by the spin-

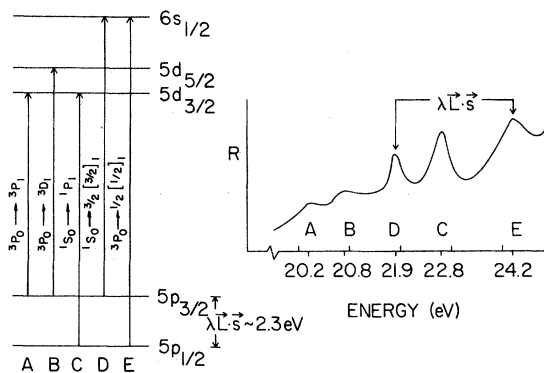


FIG. 9. Atomic model for transitions from a rare-earth 5*p* level to 5*d* and 6*s* levels. The closed-shell initial state (¹*s*₀) is labeled with the description of the whole state in *L-S* coupling. Final states are labeled in *L-S* (5*d*) or *J-j* (6*s*) notation. The transitions are identified on the reflectance spectrum of LaF₃, but this identification is not correct (see text).

orbit splitting of the 5*p* level, although in the solid the splitting may be altered by exchange effects²⁹ and the crystal field.³⁰ In the crystal, these two pairs are split by different amounts, and the pair D-E exhibits an anisotropy, becoming much weaker, and perhaps shifting to higher energy for *E* ⊥ *c*. The other three peaks appear isotropic. Anisotropy is not expected for *s*-like final states. Moreover, it is clear from the number of 4*f*-5*d* transitions that the 5*d* states are split by the crystal field, the orbital degeneracy being completely lifted because of the low site symmetry. The 5*p* → 5*d*, 6*s* spectrum in the free La³⁺ ion has been measured.^{28,31} There are five strong lines, but shifted from those found in LaF₃, and with different relative strengths and splittings. They occur at²⁸ 19.64, 22.46, 24.82, 26.77, and 27.34 eV, the spin-orbit splitting being 2.52 eV.

Crystal-field effects on such transitions have been studied previously in detail only in the simpler case of the excitation of Na⁺ 2*p*, K⁺ 3*p*, and Rb⁺ 4*p* electrons in alkali halides.³²⁻³⁴ The very low site symmetry makes a similar study for the rare-earth trifluorides very difficult, even empirical determination of parameters having proven unsatisfactory.⁵ We conclude only that the atomic picture of Fig. 9 cannot be correct and that the crystal field must be taken into account, certainly for the 5*d* levels and possibly for the 5*p*. Exchange coupling with 4*f* electrons also may be important for all but LaF₃.²⁷

It is not clear why the structures arising from the lanthanide 5*p* levels are sharper in LaF₃ than in any of the other materials studied. The excited state could interact with 4*f* electrons in the

other salts, but this should yield fluorescence. A luminescence excitation peak is observed at 22 eV in PrF_3 , but the excitation curve does not resemble the reflectance spectrum. An Auger process also could broaden these structures, but it should require two $4f$ electrons, and thus be inoperative for CeF_3 , which does not show well-resolved structures. Moreover, there is no decrease in sharpness with increasing number of $4f$ electrons beyond the first $4f$ electron. Interatomic Auger processes are expected to be less likely, and should not depend so much on lanthanide. That luminescence from $4f$ electrons does occur is indicative of coupling between the excited states, presumably $5d$ and $6s$, both of which are known to produce excitations of $4f$ electrons,⁴ and the $4f$ system. This luminescence did not distort the reflectance measurements in this spectral region. A detector blind to such emissions was used as a check. The degree of localization of the final states is not clear, for excitation of both localized $5d$ and $6s$ and bandlike states are known to produce luminescence of the $4f$ system.

The absorption spectra for metallic Pr (Ref. 35) and Gd (Ref. 36) show single peaks at 25 and 21 eV, respectively, without spin-orbit splitting. The fact that this peak is almost the same for Pr and PrAl_2 (Ref. 35) strongly suggests that the $5p$ - $5d$ transitions are highly localized on the atomic site. In the corresponding trifluorides there are certainly crystal-field effects on these transitions arising from the F^- neighbors, but it is not clear how localized the final states are. One expects more localization near threshold.

The next major structure is the large reflectance peak that moves from 27.0 eV in LaF_3 to 29.5 eV in NdF_3 , and to still-higher energy in GdF_3 . The magnitude of this peak is remarkable. Single crystals of these salts are better reflectors in this spectral region than any metal known. Because of the shift to higher energy with increasing atomic number, we identify this as the "interband" transition from the lanthanide $5p$ levels to the conduction band. Similar peaks are seen in the electron energy loss spectra of the heavy rare earths.^{37,38} The thresholds, however, are at lower energies that do not increase monotonically with increasing atomic number, but scatter somewhat. As such, it should represent the density of conduction-band states, weighted by the square of the dipole matrix element, but probably with little or no effect of the electron-hole interaction. There is very little anisotropy in the peak position. Most of the salts studied also have a shoulder on the high-energy side of this peak, which appears more prominently in the $\vec{E} \parallel \hat{c}$ spectra, although this is at the limit of re-

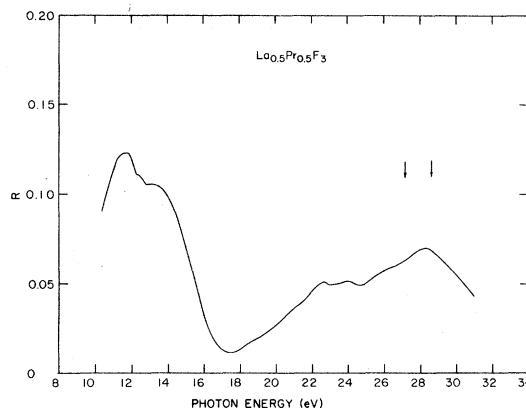


FIG. 10. Reflectance of a polycrystalline sample of $\text{La}_{0.5}\text{Pr}_{0.5}\text{F}_3$.

liability because of possible artifacts of surface preparation. The separation of this from the main peak is about that of the splitting of the two main peaks in the 10–15-eV spectra, a splitting due to the conduction-band structure. This splitting is too large to ascribe the shoulder to excitations of the lanthanide $5s$ levels, for XPS data²⁴ show that these lie at least 20 eV below the lanthanide $5p$ levels, the separation increasing with atomic number. (It normally would not be very safe to discuss splittings in a reflectance spectrum, because they may differ appreciably from the splittings in the ϵ_2 spectra, but in this region the two spectra are nearly the same for LaF_3 ,⁷ and the spectra of the other materials we have measured are nearly the same as that of LaF_3 .) These transitions are relatively weak. In the 15–30-eV region, about 1.8 electrons per molecule contribute to the partial sum rule on ϵ_2 for PrF_3 . Because of the highly localized initial states, the oscillator strength is spread over a wide energy range.

Figure 10 shows the reflectance spectrum of a polycrystalline sample of $\text{La}_{0.5}\text{Pr}_{0.5}\text{F}_3$, a sample whose reflectance is low because of poor sample surface quality, which was difficult to judge because of the graininess of the interior. It was hoped to resolve two peaks in the 25–30-eV region, demonstrating the additivity of the transitions because of their highly localized initial states and nearly identical final states. The arrows show these expected peak positions, but two peaks have not really been resolved.

SUMMARY

Transmission measurements show the $4f \rightarrow 5d$ and $4f \rightarrow 6s$ transitions are similar to those of the rare-earth ions doped into LaF_3 . The reflectance

spectra show strong interband absorption in the 10–15-eV region, presumably from the $F^- 2p$ valence band to lanthanide $5d$ and $6s$... conduction bands. There is, surprisingly, no evidence for excitons, even in LaF_3 , which is transparent until the onset of interband transitions. The valence band \rightarrow conduction band transitions continue weakly to very high energies. Lanthanide $5p \rightarrow 5d$ transitions occur above 20 eV. At their onset, the discrete final states show strong evidence of crystal-field effects, for anisotropy occurs. Finally, $5p$ transitions to the conduction bands give a very large reflectance above 27 eV. More insight about the states involved could be obtained

from a thorough study of fluorescence in these materials.

ACKNOWLEDGMENTS

This work was carried out at the Synchrotron Radiation Center, Physical Sciences Laboratory of the University of Wisconsin (supported by NSF Contract No. DMR W-7405-eng-82). The assistance of the staff is gratefully acknowledged. The crystals were kindly provided by P. E. Palmer and B. J. Beaudry of the Ames Laboratory. This work was supported by the U. S. Department of Energy, Division of Basic Energy Sciences.

- *Present address: Gruppo Nazionale di Struttura della Materia del Consiglio Nazionale delle Ricerche, Sezione di Roma, Istituto di Fisica della Università, Rome, Italy.
- ¹R. W. G. Wyckoff, *Crystal Structure* (Interscience, New York, 1963), Vol. II.
 - ²R. P. Lowndes, J. F. Parrish, and C. H. Perry, *Phys. Rev.* **182**, 913 (1969).
 - ³P. R. W. Hudson, *J. Phys. C* **9**, L39 (1976).
 - ⁴L. R. Elias, W. S. Heaps, and W. M. Yen, *Phys. Rev. B* **8**, 4989 (1973).
 - ⁵W. S. Heaps, L. R. Elias, and W. M. Yen, *Phys. Rev. B* **13**, 94 (1976).
 - ⁶D. W. Lynch and C. G. Olson, *Solid State Commun.* **12**, 661 (1973); C. G. Olson, M. Piacentini, and D. W. Lynch, in *Vacuum Ultraviolet Radiation Physics*, edited by E. E. Koch, R. Haensel, and C. Kunz (Pergamon-Vieweg, Braunschweig, 1975), p. 411.
 - ⁷G. Stephan, M. Nisar, and A. Roth, *C. R. Acad. Sci. B* **274**, 807 (1972).
 - ⁸M. Nisar, A. Roth, G. Stephan, and S. Robin, *Opt. Commun.* **8**, 254 (1973).
 - ⁹F. H. Spedding and D. C. Henderson, *J. Chem. Phys.* **54**, 2476 (1971).
 - ¹⁰C. G. Olson and D. W. Lynch, *Phys. Rev. B* **9**, 3159 (1974).
 - ¹¹A. J. Popov and G. E. Knudson, *J. Am. Chem. Soc.* **76**, 3921 (1954).
 - ¹²E. V. Sayre and S. Freed, *J. Chem. Phys.* **23**, 2066 (1955).
 - ¹³S. S. Batsanov, S. S. Derbeneva, and L. R. Batsanova, *Zh. Prikl. Spektrosk.* **10**, 332 (1969) [*Sov. Phys.-J. Appl. Spect.* **10**, 240 (1969)].
 - ¹⁴R. Solomon and L. Mueller, *Appl. Phys. Lett.* **3**, 135 (1963).
 - ¹⁵W. R. Hunter and S. A. Malo, *J. Chem. Phys. Solids* **30**, 2739 (1964).
 - ¹⁶J. B. Mooney, *Infrared Phys.* **6**, 153 (1966).
 - ¹⁷G. H. Diecke and H. M. Crosswhite, *Appl. Opt.* **2**, 675 (1963).
 - ¹⁸E. Loh, *Phys. Rev.* **147** 332 (1966).
 - ¹⁹M. Schlesinger and T. Szczurek, *Phys. Rev. B* **8**, 2367 (1973).
 - ²⁰G. K. Wertheim, A. Rosenczweig, R. L. Cohen, and H. J. Guggenheim, *Phys. Rev. Lett.* **27**, 505 (1971).
 - ²¹W. Van Gool and A. G. Piken, *J. Mater. Sci.* **4**, 95 (1969).
 - ²²S. Sato, Y. Sakisaka, and T. Matsukawa, in Ref. 6, p. 414.
 - ²³W. Pong and C. S. Inouye, *J. Opt. Soc. Am.* **68**, 521 (1978).
 - ²⁴D. W. Lynch (unpublished).
 - ²⁵J. A. Bearden and A. F. Burr, *Rev. Mod. Phys.* **39**, 128 (1967).
 - ²⁶F. Herman and S. Skillman, *Atomic Structure Calculations* (Prentice-Hall, Englewood Cliffs, New Jersey, 1963).
 - ²⁷R. L. Cohen, G. K. Wertheim, A. Rosenczweig, and H. J. Guggenheim, *Phys. Rev. B* **5**, 1037 (1972).
 - ²⁸J. Reader and G. L. Epstein, *J. Opt. Soc. Am.* **65**, 638 (1975).
 - ²⁹Y. Onodera and Y. Toyozawa, *J. Phys. Soc. Jpn.* **22**, 833 (1967).
 - ³⁰L. Ley, S. P. Kowalczyk, F. R. McFeely, and D. A. Shirley, *Phys. Rev. B* **10**, 4881 (1974).
 - ³¹J. Comerade, W. R. S. Garton, M. W. P. Mansfield, M. A. P. Martin, F. S. Tomkins, and D. H. Tracy (unpublished).
 - ³²T. Åberg and J. L. Dehmer, *J. Phys. C* **6**, 1450 (1973).
 - ³³C. Satoko and S. Sugano, *J. Phys. Soc. Jpn.* **34**, 701 (1973).
 - ³⁴C. Satoko, *Solid State Commun.* **13**, 1851 (1973).
 - ³⁵H. J. Hagemann, W. Gudat, and C. Kunz, *Phys. Status. Solidi B* **74**, 507 (1976).
 - ³⁶B. Loisel, A. Quemerai, M. Priol, and S. Robin (unpublished).
 - ³⁷B. Brousseau, J. Frandon, C. Colliex, P. Trebbia, and M. Gasgnier, in Ref. 6, p. 622.
 - ³⁸C. Colliex, M. Gasgnier, and P. Trebbia, *J. Phys. (Paris)* **37**, 397 (1976).